[CANCER RESEARCH 59, 558–564, February 1, 1999]

Identification of Functional Elements of $p18^{INK4C}$ Essential for Binding and Inhibition of Cyclin-dependent Kinase (CDK) 4 and CDK6[1]

Seong J. Noh, Yan Li, Yue Xiong, and Kun-Liang Guan[2]

Department of Biological Chemistry and the Institute of Gerontology, University of Michigan Medical School, Ann Arbor, Michigan 48109-0606 [S. J. N., K-L. G.]; and Department of Biochemistry and Biophysics, University of North Carolina, Chapel Hill, North Carolina 27599-7295 [Y. L., Y. X.]

ABSTRACT

Members of the INK4 family of cyclin-dependent kinase (CDK) inhibitors specifically bind and inhibit the G_1-specific CDK molecules CDK4 and CDK6. One of the INK4 molecules, p16, is also known as multiple tumor suppressor and has been found to be mutated or deleted in various tumors and cell lines. We have previously identified p18 as a member of the INK4 family. To determine the molecular basis for the inhibitory function of p18, we introduced 11 missense mutations of conserved residues that were identified in p16 of cancer cell lines into p18. The effects of these mutations on the ability of p18 to bind and inhibit CDK4 and CDK6 or to inhibit cell growth were determined. Our results indicate that the third ankyrin repeat and the NH_2-terminal portion of the fourth repeat constitute the essential element necessary for the ability of p18 to bind and inhibit CDK4 and CDK6. Apart from this core interaction element, p18 seems to use additional, distinct residues to differentially bind and inhibit CDK4 and CDK6, accounting for the known penchant of p18 to preferentially interact with CDK6.

INTRODUCTION

The molecular engines that propel mammalian cells through the first gap phase into S phase are: the G_1-specific CDKs[3] CDK4 and CDK6, in complexes with their regulatory subunits, cyclin D1, D2, and D3; and CDK2, in complex with cyclin E (1). Of the numerous modes of regulation that impinge upon the cyclin D-associated CDK activity, two classes of CDK inhibitors exist. The first class of inhibitors, which consists of p21 (WAF1/Cip1), p27 (Kip1), and p57 (Kip2) is able to bind and inhibit all known cyclin-CDK complexes (2–6). On the other hand, the INK4 family, which consists of $p15^{INK4B}$, $p16^{INK4A}$, $p18^{INK4C}$, and $p19^{INK4D}$, specifically interacts with and inhibits the cyclin D-CDK4 and cyclin D-CDK6 complexes (7–12).

Although ample evidence exists that INK4 molecules share similar biochemical properties, namely, binding and inhibiting the activity of cyclin D-dependent CDK molecules (7, 8, 13), the exact physiological functions of each of the INK4 molecules are not well defined. It is postulated that p16 may function to inhibit CDK4/6 activity during S, G_2, and M phases, at which time the kinase activity may be detrimental to the cell (7). In the macrophages and other hematopoietic cells, in which p16 is known to be absent (11, 14), p18 and p19 levels drop during G_1 and accumulate as the G_1-S boundary is reached (11), possibly substituting for p16 function. Yet another role of INK in cell cycle is suggested by the induction of p15 expression upon transforming growth factor-β stimulation in human epithelial cell line (9) mediating transforming growth factor-β-induced G_1 arrest. The varied functions of the INK4 molecules may result from the probable differential affinities between the various cyclin D-CDK holoenzymes and particular INK4 molecules (8) and also the differential tissue expression of the INK4 family members (9, 11, 14).

$p16^{INK4A}$ is also known as multiple tumor suppressor because mutations in this gene were documented in a wide variety of tumors and cell lines (15). Deletions of 9p21, the chromosomal region that includes p16, were reported for lung and bladder carcinomas, acute lymphoblastic leukemias, melanomas, pancreatic adenocarcinomas, and gliomas. Most of the reported mutations were frameshift or nonsense mutations; however, a handful of missense mutations were also reported (15–21). *In vitro* characterization of some of these p16 missense mutants revealed that some of the mutations caused complete loss of CDK4 inhibitory activity, whereas others did not affect inhibition at all (13, 22–26). The majority of the loss of function mutants of p16 identified in these studies, such as H83Y, R87P, P114L, and V126D, involved residues that are conserved between the INK4 family members. In contrast, mutations of nonconserved residues, such as I49T, N71S, A127S, and A148T, did not affect the inhibitory function of p16. The fact that the loss of function mutants of p16 involve conserved residues is significant, given that the INK4 family members share very low amino acid sequence identity (~30%) and that these rare, conserved residues occur in clusters (Fig. 1). These clusters of conserved residues, therefore, might constitute critical structural or functional elements of the INK4 family.

As alluded to above, p18 may quite possibly serve a physiological function different from that of p16. Two lines of evidence further support this idea. (*a*) The frequency of deletion or mutations of p18 in cancer tissues is very low compared to that of p16 (27, 28). (*b*) *In vivo* coimmunoprecipitation experiments demonstrated that p18 preferentially associates with CDK6, whereas p16 associates with both CDK4 and CDK6 (8). In light of these observations, we wished to determine the possible biochemical basis for the functional differences between p16 and p18. Because the clusters of conserved residues of p18 likely constitute elements critical for the inhibitor's function, biochemical characterization of the mutants of these conserved residues was expected to garner insights into the molecular mechanism of the function of p18. By selectively mutating conserved residues of p18 that span the entire molecule, we hoped to attain a clearer identification of functional modules of the inhibitor.

To achieve this end, we produced 11 mutants of p18, each (except for one) with a mutation of a single conserved residue corresponding to that found in p16 of cancer tissues. Biochemical characterization of the eleven mutants revealed that the third ankyrin repeat of p18, along with the NH_2-terminal portion of the fourth ankyrin repeat, is critical for the biochemical activity of p18. Some mutants displayed differential binding affinities toward CDK4 and CDK6, suggesting a possible mode by which p18 discriminates between the two G_1-specific CDK molecules.

MATERIALS AND METHODS

Cell Culture. Both U-2OS and SaOS cells (human osteosarcoma cell lines) were maintained in DMEM supplemented with 10% fetal bovine serum. Cells were cultured in a 37°C incubator with 5% CO_2.

Mutagenesis and Purification of Mutant Proteins. The full coding sequence of p18 (8) was subcloned into pALTER mutagenesis vector (Promega), and the oligonucleotide-directed mutagenesis was achieved according to recom-

Received 8/7/98; accepted 11/23/98.

The costs of publication of this article were defrayed in part by the payment of page charges. This article must therefore be hereby marked *advertisement* in accordance with 18 U.S.C. Section 1734 solely to indicate this fact.

[1] This work was supported by NIH Grant GM 51586 and the Taisho Excellence in Research Program (to K-L. G.) and NIH Medical Scientist Training Grant 5T32GM07863 and NIH Pharmacological Sciences Training Program Grant 5T32GM07767 (to S. J. N.).

[2] To whom requests for reprints should be addressed, at Department of Biological Chemistry, University of Michigan Medical School, Room 4432, Medical Science I, Ann Arbor, MI 48109-0606. Phone: (313) 763-3030; Fax: (313) 763-4581; E-mail: Kunliang.guan@umich.edu.

[3] The abbreviations used are: CDK, cyclin-dependent kinase; GST, glutathione *S*-transferase; FACS, fluorescence-activated cell sorting.

mended protocol (Promega). Mutants were confirmed by sequencing (United States Biochemical). Confirmed mutant p18 clones were then subcloned into pGEX-KG vector (29), and the resulting pGEX-KG-p18 (or mutant) plasmid was transformed into BL21 strain of *Escherichia coli.* These transformed cells were cultured and used for purification of the GST-tagged p18 protein using glutathione-agarose affinity resin as detailed by Guan and Dixon (29).

***In Vitro* CDK6 Activity Assay.** The assays used to determine the kinase activity of CDK4 and CDK6 were identical except for the use of the appropriate kinase subunit. The activity assay will be described for CDK6. Recombinant CDK6 and cyclin D2 were expressed as NH_2-terminal GST fusion proteins and were purified by a method identical to that described above for GST-p18. For use as substrate, the COOH-terminal 137 amino acid residues of pRb was also expressed as GST-fusion protein and purified as described above. For each kinase reaction, lysate of $\sim 3 \times 10^5$ exponentially growing Jurkat cells [in CAK buffer: 80 mM sodium β-glycerophosphate, 15 mM $MgCl_2$, 1 mM benzamidine, and 0.1 mM orthovanadate in 5 mM HEPES (pH 7.4), supplemented with 5 μg/ml leupeptin, 3.5 μg/ml aprotinin, 0.5 mM phenylmethylsulfonyl fluoride, and 10 mM DTT] was mixed with 0.2 μg of GST-CDK6 and 0.2 μg of GST-cyclin D2 in the presence of 1 mM ATP. This activation was allowed to proceed for 1 h at room temperature. After incubation, 5 μl of 50% (v/v) glutathione agarose beads per kinase reaction were used to affinity purify the activated GST-CDK6/GST-cyclin D2 complex. The activated kinase complex was eluted in 10 μl of kinase buffer [50 mM HEPES (pH 7.0) with 10 mM $MgCl_2$, 5 mM $MnCl_2$, 1 mM DTT, and 0.1 mM ATP] containing 10 mM glutathione. The eluent containing the activated complex was mixed with 2.5 μg of GST-Rb, 10 μCi of [γ-^{32}P]ATP, and 4 μl of 5-fold concentrated kinase buffer to a final volume of 20 μl. This kinase reaction mixture was incubated for 1 h at 30°C. Half of the reaction mixture was analyzed by SDS-PAGE and autoradiography.

To assess the inhibition of CDK6 by p18 or mutant, we diluted the predetermined amount of inhibitor (see Fig. 2) to a final volume of 5 μl with 25 mM HEPES (pH 7.0) and added the solution to the kinase reaction mixture.

IC_{50}s for the mutants were determined using the pseudo-Hill plot. A PhosphorImager (Molecular Dynamics) was used to quantitate the intensities of the phosphorylated Rb bands. Highest intensity value for each set of data (*e.g.*, CDK6 inhibition by 0, 10, 30, 100, 300, or 1000 ng of p18), was set to be 100% activity. The percentage of activity remaining at each inhibitor (p18 or mutant) concentration was defined to be *p*, the percentage competition of specific binding in the presence of a set concentration of inhibitor. A plot of $\log [p/(100 - p)]$ *versus* $\log [I]$, where $[I]$ is the concentration of inhibitor, yielded a linear plot. The r^2 values for all sets of data ranged between 0.78 to 0.95. IC_{50}s were derived from the following equation:

$$\log [p/(100 - p)] = n \log [I] + n \log IC_{50}$$

***In Vitro* Binding Assay.** Full-length coding sequences of CDK4 and CDK6 were subcloned into the pT7-7 vector for use as a DNA template in the *in vitro* transcription. [^{35}S]Methionine-labeled CDK4 and CDK6 were synthesized *in vitro* using the T7 RNA polymerase-driven TNT-coupled reticulocyte lysate system (Promega). For each binding reaction, 1/12 of the [^{35}S]methionine-labeled CDK4 or CDK6 was mixed with varying volumes of bacterial lysate containing 1 μg of GST (or GST-p18 or mutant), 40 μl of 50% (v/v) glutathione agarose beads, and NETN buffer to a final volume of 400 μl. The binding reaction mixtures were gently mixed at 4°C for 1 h. The beads were washed three times with 1 ml of NETN (100 mM NaCl, 1 mM EDTA, 20 mM Tris ph 8.0, 0.5% NP-40, 0.5 mM Na_3VO_4, 50 nM Naf, 0.2 mM phenylmethylsulfonylfluoride, 1 μg/ml leupeptin) buffer. To the washed beads were added 20 μl of SDS sample buffer, and the mixture was vortexed and boiled for 5 min to extract the proteins bound to the beads. The supernatant was resolved on denaturing polyacrylamide gel for SDS-PAGE analysis followed by autoradiography.

Saturation Binding Experiments. Wild-type p18 and two representative mutants, A61T and D76N, were expressed and purified to near homogeneity as untagged recombinant proteins. ^{35}S-labeled p18 was produced using the *in vitro* coupled transcription-translation system (Promega). An aliquot of the labeled p18 (p18*) was mixed with varying concentrations of the cold, untagged p18 in the presence of GST-CDK6/GST-cyclin D2 complex, and the mixture was allowed to incubate for 2 h to allow equilibrium binding. The complex formed was precipitated using glutathione agarose and resolved on a 15% SDS-polyacrylamide gel (Fig. 4). A PhosphorImager was used to quantitate the intensity of the p18* band, which represented the amount of labeled p18 remaining bound to the GST-CDK upon competition with cold p18. The concentration of cold, untagged p18 (or mutant) that caused the dissociation of 50% of the labeled p18 from the CDK6-cyclin D2-p18 complex was taken to be an estimate of the apparent K_D.

Cyclin D2 Displacement Assay. GST-cyclin D2 (10 ng) was incubated with 5 μl of *in vitro* translated CDK6 in the presence of varying concentrations of untagged, purified p18 (wild-type, A61T, or D76N). The mixture was incubated at 30°C for 30 min and then immunoprecipitated using anti-cyclin D1 antiserum that is known to cross-react with cyclin D2. The immunoprecipitated complex was extensively washed with TNE buffer [10 mM Tris (pH 7.5), 2 mM EDTA, 100 mM NaCl, 1% NP40, and 50 mM NaF] and solubilized with 40 μl of SDS-PAGE sample buffer. Half of this sample was resolved on SDS-polyacrylamide gel and autoradiographed.

Cell Cycle Analysis. Full length coding sequences of p18, A61T, D76N, Q93W, and D100Y were subcloned into pcDNA3 vector (Invitrogen), behind the CMV promoter. pCMV-CD20 was a generous gift from Dr. E. Harlow (30). U-2OS cells grown to log phase were seeded at a density of 5×10^5 cells per 10 cm tissue culture dish 1 day prior to transfection. Plasmids encoding wild-type or mutant p18 was cotransfected into the cells with pcDNA3-CD20 using Lipofectamine (Life Technologies, Inc.). After a 48-h incubation at 37°C, cells were washed with PBS and detached using PBS containing 0.1% EDTA (v/v). Detached cells were then incubated with FITC-conjugated anti-CD20 antibody for immunofluorescence staining of transfected cells. Cells were then fixed and stained with propidium iodide for nuclear staining. Red fluorescence, as a measure of DNA content, and green fluorescence, as a measure of CD20 expression level, were analyzed by double-gated FACS analysis.

Colony Formation Assay. Colony formation assay was performed as described previously (31). Full-length coding region of wild type (both sense and antisense orientation) or mutant p18 was subcloned into pcDNA3 (Invitrogen). U-2OS cells were transfected with 2 μl of the appropriate plasmid construct, using Lipofectamine (Life Technologies, Inc.), and maintained in the normal growth medium (DMEM plus 10% fetal bovine serum) for 2 days. Cells were then split at various dilutions to 10-cm plates and cultured in medium supplemented with 500 μg/ml G418 (Life Technologies, Inc.) for 2–3 weeks, with change of medium every 4–5 days. G418-resistant colonies consisting of >50 cells were counted at the end of 2–3 weeks.

Western Blot of Transfection Samples. U-2OS cells were transfected as described above. Two days after transfection, cells were lysed with 100 μl of PBS containing 0.1% Triton. Protein content of the lysate was determined using modified Bradford protein assay (Bio-Rad). The volume of each lysate sample containing approximately 30 μg of protein were loaded onto 15% SDS gel, and the sample was resolved by SDS-PAGE. The proteins were then transferred to nitrocellulose filter paper, and the blot was probed with anti-p18 antiserum (8), followed by horseradish peroxidase-conjugated antirabbit IgG antibody. The reacting p18 band was detected using enhanced chemiluminescence reagent (Amersham).

RESULTS

***In Vitro* CDK6 Activity Assays.** To determine the effect of each mutation on the ability of p18 to inhibit CDK6, we performed an *in vitro* CDK6 activity assay in the presence of varying concentrations of the GST fusion protein with wild-type or mutant p18. Although mutations at G16, Q93, and A110 minimally affected the CDK6 inhibitory function of p18, mutations at the central cluster of residues in the third ankyrin repeat (D76, R79, L89, and D100) drastically reduced the ability of p18 ability to inhibit CDK6 (Figs. 1 and 2*b*). For example, D76N did not significantly inhibit CDK6 activity, even at 1000 ng, whereas 30 ng of wild type p18 almost completely inhibited CDK6 activity. For a more quantitative measure of the loss of inhibition, IC_{50}s for the wild-type and mutant p18 were determined using PhosphorImager-derived quantification of the intensities of the phosphorylated Rb bands (Table 1). It is clear from comparison of the IC_{50}s that mutations of residues D76, R79, L89, or D100 caused the most severe reduction ($>$50-fold) in the potency of p18 as CDK6 inhibitor. These results suggest that the residues in the third ankyrin repeat are essential for the ability of p18 to inhibit CDK6 activity. The only mutant deviating from this trend was Q93W, which is the only

```
                                       D
P18              MAEPW.GNELS SAAARGDLEQ LTSLLQNN.VN      30
P19            ML LEEVRAGDRLS GAAARGDVQE VRRLLHRELVH     34
P16       MDPPAG SSMEPSADWLA TAAARGRVEE VRALLE.AVAL      37
                                   1

                                           T
p18    VNAQNGFGRT ALQVMKLGNP EIARRLLLRG ANPDLKDRTG       70
P19    PDALNRFGKT ALQVMMFGST AIALELLKQG ASPNVQGTSG       74
P16    PNAPNSYGRR PIQVMMMGSA RVAELLLLHG AEPNCADPAT       77
                         2

          N  P  S      P    W      Y    L  S
P18    FA.VIHDAARA GFLDTLQTLL EFQADVNIED NEGNLPLHLA      110
P19    TS.PVHDAART GFLDTLKVLV EHGADVNVPD GTGALPIHLA      114
P16    LTRPVHDAARE GFLDTLVVLH RAGARLDVRD AWGRLPVDLA      118
                3

         D
P18    AKEGHLRVVE FLVKHTASNV GHRNHKGDTA CDLARLYGRN       150
P19    VQEGHTAVVS FLA..AESDL HRRDARGLTP LELALQRGAQ       152
P16    EELGHRDVAR YLRAAAGGTR GSNHARIDAA EGPSDIPD         156
             4

P18    EVVSLMQANG AGGATNLQ                               168
P19    DLVDILQGHM VAPL                                   166
```

Fig. 1. Sequence alignment of INK4 members p16, p18, and p19. Residues in *boldface* are strictly conserved. *Italicized letters* represent the amino acid residue substitution made in the p18 sequence for mutational analysis in this study. *Solid lines* indicate the extents of the tandem ankyrin repeats in the molecules.

mutant tested that involved a nonconserved residue (Q93 is glycine in both p16 and p19). It is also noteworthy that mutations of some of the residues that flank the third ankyrin repeat also caused substantial reduction in the ability of p18 ability to inhibit CDK6. A61T, P106L, and V118D were 11-, 16-, and 11-fold less potent than wild-type p18 as CDK6 inhibitor (Figs. 1 and 2*b*; Table 1).

SDS-PAGE analysis followed by Coomassie blue staining revealed that all mutants were stable to purification and storage conditions. Only L89P and V118D suffered significant degradation, suggesting possible structural alterations. Therefore, it is unlikely that the loss of inhibition observed in all mutants is due to gross structural changes.

***In Vitro* CDK4 Activity Assays.** It has been shown previously that p18 interacts more strongly with CDK6 than with CDK4 *in vivo* (8). Therefore, we were interested in determining whether the various mutations would differentially affect the ability of p18 to inhibit CDK4 and CDK6. An *in vitro* activity assay similar to that for CDK6 was performed using CDK4. Results (Fig. 2; Table 1) indicate that each of the mutants exhibited similar levels of inhibition toward both CDK4 and CDK6. This suggests that common structural elements of p18 are required for inhibition of both CDK4 and CDK6.

***In Vitro* Binding Assays.** The loss of inhibitory function of the various mutants could be due to one or both of two factors. The mutated residue may be critically involved in the inhibition itself or the mutation may prevent proper binding of p18 to the CDK molecule. To distinguish between these two possibilities, the ability of each mutant to bind to CDK4 or CDK6 was tested by *in vitro* binding assay. The most striking result of the *in vitro* binding experiments was that two of the mutants, D76N and D100Y, did not bind to CDK6 at all (Fig. 3; Table 1). Mutation of other residues within the third ankyrin repeat (R79, L89, and Q93) and P106 of the fourth repeat also caused a significant loss of binding (Fig. 3). This result indicates that residues D76 and D100 are essential for binding of p18 to CDK6. The entire third ankyrin repeat and the NH_2-terminal portion of the fourth repeat also seem to contribute to CDK6 binding.

With regard to CDK4, the mutant D100Y was unable to bind to the CDK molecule, just as was observed for CDK6 binding. R79P was also similarly unable to bind to CDK4. Surprisingly, mutations of D76 and other residues in the third ankyrin repeat (G81, L89, and Q93) did not affect CDK4 binding, in contrast to the results for CDK6. This suggests that p18 may use both common and distinct attributes of the third ankyrin repeat to specifically bind to CDK4 or CDK6. Still more interesting is the observation that D76N retained CDK4 binding ability, yet was completely inactive as an inhibitor. This observation suggests that aspartate 76 has a critical role in CDK inhibition.

Saturation Binding. Although activated holoenzyme CDK-cyclin D2 complex was used for assessing the ability of the mutants to inhibit the Rb kinase activity of CDK4 or CDK6, the *in vitro* binding assays were performed in the absence of cyclin D2. Saturation binding experiments were performed to corroborate the *in vitro* binding data in the context of holoenzymes.

The concentration of cold, untagged p18 that caused the dissociation of 50% of the labeled wild-type p18 from the CDK6-cyclin D2-p18 complex, which is an estimate of the apparent K_D, was determined to be 55 nM. The apparent K_D for A61T binding to the CDK6-cyclin D2 complex was 250 nM (Fig. 4). The same analysis was carried out using D76N but did not yield useful data because the labeled D76N did not bind to CDK6 or CDK6-cyclin D2 complex at a detectable level (data not shown). The lack of binding of labeled D76N to CDK6-cyclin D2 complex is completely consistent with the results of the *in vitro* binding experiment described above. The same experiments were attempted using GST-CDK4-GST-cyclin D2 complex. Whereas CDK6-D2 complex precipitated an easily detectable and quantifiable level of labeled p18 and A61T, the CDK4-D2 complex precipitated much less labeled p18 (data not shown). The amount of labeled p18 that was precipitated with CDK4 was so low that reliable PhosphorImager quantitation could not be obtained. Again, this observation is entirely consistent with the previously reported *in vivo* data that p18 preferentially forms a complex with CDK6.

Cyclin D2 Displacement Assay. Addition of free p16 to preformed CDK4-cyclin D1 complex or to a mixture of CDK4 and cyclin

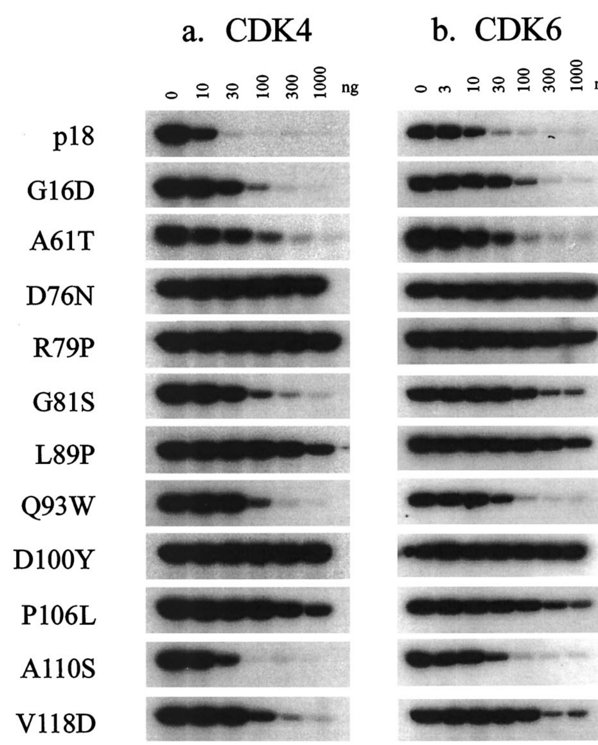

Fig. 2. *In vitro* CDK4/CDK6 activity assay. Recombinant Rb fragments were used as substrates for the activated complexes of cyclin D2-CDK4 or cyclin D2-CDK6. Each panel represents autoradiographed image of ^{32}P-phosphorylated Rb from the activity of CDK4 (*a*) or CDK6 (*b*) in the presence of wild-type or mutant p18 (labeled on the *left*) in the amounts indicated on top (ng), except for A61T, for which 0, 10, 20, 50, 100, and 500 ng were used for CDK4 and 0, 10, 20, 50, 100, 500, and 1000 ng were used for CDK6 activity assays.

Table 1 *Inhibitory and binding capacity of the wild-type p18 and mutants toward CDK4 or CDK6*[a]

	CDK4		CDK6	
	IC_{50} (nM)	Binding	IC_{50} (nM)	Binding
p18	10	+++	10	+++
G16D	30	+++	40	+++
A61T	100	+++	110	+++
D76N	>1000	++	>500	−
R79P	>1000	+	>500	+
G81S	20	+++	100	+++
L89P	510	+++	>500	+
Q93W	50	+++	30	+
D100Y	>1000	+	>500	−
P106L	260	+++	160	+
A110S	20	+++	20	++
V118D	60	+++	110	++

[a] IC_{50}s were derived from the quantification of intensity of phosphorylated Rb bands relative to concentration of inhibitor (Fig. 2). Scores for binding ability of the wild-type or mutant p18 are derived from the intensity of ^{35}S-labeled CDK4 or CDK6 band (Fig. 3). +++, 90–100% of wild type; ++, 50–89% of wild type; +, 10–49% of wild type; −, 0–9% of wild type. Identities of the inhibitors are shown in the far left column.

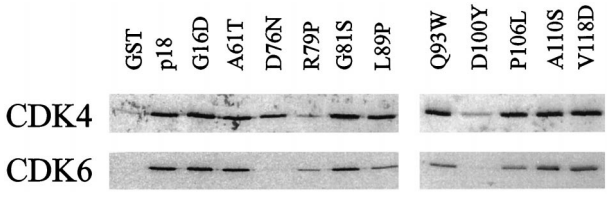

Fig. 3. *In vitro* binding assay. *In vitro* translated, ^{35}S-labeled CDK4 or CDK6 was allowed to interact with GST-p18 wild type or mutant, as indicated on *top*. The bands represent the amount of radioactive CDK4 or CDK6 recovered on glutathione-agarose resin from each reaction mixture.

D1 was shown to disrupt CDK4-cyclin D1 complex formation, concomitant with the accumulation of CDK4-p16 complex (32, 33). To assess whether p18 also acts by displacing cyclin D from CDK-cyclin D complex, cyclin D2 displacement assay was performed (Fig. 5). Our data indicate that addition of wild-type p18 causes efficient dissociation of cyclin D2 from CDK6 (Fig. 5). D76N, which does not bind CDK6 well, displays much diminished ability to displace cyclin D2 from CDK6, whereas A61T shows an intermediate displacement of cyclin D2. These results correlate well with the CDK binding affinities determined by the two binding experiments (Figs. 3 and 4).

Effects of the p18 Mutants on Cell Cycle. Having assessed the effects of the various mutations on the biochemical function of p18, we wished to test the effects of the mutations on the ability of p18 to control cell cycle *in vivo*. Representative mutants A61T, D76N, Q93W, and D100Y, as well as the wild-type p18, were subcloned into a eukaryotic expression vector, pcDNA3. These constructs were then cotransfected into U-2OS cells, a human osteosarcoma cell line known to express functional Rb protein, along with a vector encoding the surface marker CD20 as a transfection control. The DNA contents of CD20-positive cells were analyzed by two-parameter flow cytometry (Fig. 6).

In wild-type p18-transfected cells, significantly larger percentage of cells were found to be in G_1 relative to vector-transfected controls (47 ± 7% and 25 ± 7%, respectively, Table 2; Fig. 6). Similar results were observed for cells transfected with pcDNA3-A61T (51 ± 10%) or Q93W (48 ± 11%), whereas transfection with pcDNA3-D76N or D100Y did not result in G_1 arrest (29 ± 10% and 16 ± 10%, respectively). Western blot of the transfection samples confirmed that all mutants were expressed (Fig. 7), affirming that the failure to cause G_1 arrest is an attribute of the mutant and not a function of expression level. To ascertain that these cell cycle effects are due to the inhibition of D-type CDK activity, the same vectors were transfected into SaOS cells, an osteosarcoma cell line that is missing functional Rb. In these cells, wild-type p18, A61T, and Q93W did not cause a build-up of G_1 population relative to controls (data not shown). The arrest of cell cycle at G_1 by p18 and the mutants is, thus, specific and dependent on functional Rb.

The effects of the various mutants on cell cycle are consistent with the *in vitro* binding and inhibition data. A61T binds well to both CDK4 and CDK6 but is a less potent inhibitor of both CDK6 and CDK4 relative to wild-type p18 (~10-fold, Table 1). In the transfection system, A61T is overexpressed. The increased concentration of the mutant inhibitor most likely compensated for the loss of potency, allowing a similar level of G_1 arrest as the wild-type p18. The same argument holds for the G_1 arrest observed in Q93W-transfected cells. D76N, on the other hand, cannot bind to CDK6 (although it can bind to CDK4) and does not inhibit either of the CDKs. Overexpression of D76N and also D100Y, as predicted from the *in vitro* data, does not cause cells to arrest at G_1.

Growth Inhibition. It has been shown previously that overexpression of wild-type p18 inhibits cell growth and proliferation in an Rb-dependent manner (8). To further demonstrate that the growth suppression of U-2OS cells by p18 is due to its ability to inhibit D-type CDK kinase activity, the effects of the various mutations on the ability of p18 ability to inhibit cell growth were determined by using the colony formation assay (31). The plasmid constructs (pcDNA3) containing wild-type p18, antisense p18, A61T, D76N, Q93W, or D100Y were transfected individually into U-2OS cells. The transfected cells were grown in medium supplemented with G418 to select for resistant colonies. Number of colonies forming in this selective media for each transfection sample was counted and com-

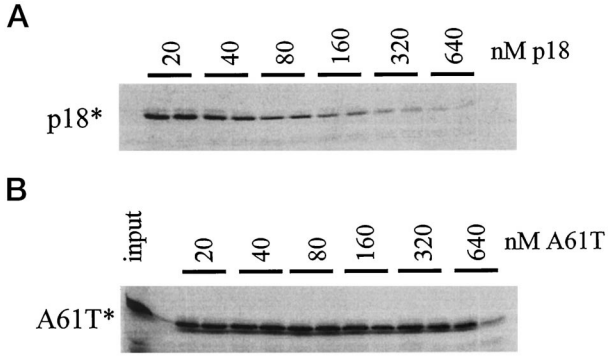

Fig. 4. Saturation binding assays. *A*, an aliquot of *in vitro* translated, ^{35}S-labeled p18 (*p18**) was bound to GST-CDK6-GST-D2 complex in the presence of varying amounts of cold, untagged p18, as indicated on *top*. The resulting complex was pulled down with glutathione agarose beads and resolved on SDS-PAGE for visualization and quantitation using a PhosphorImager. *B*, an aliquot of A61T* was bound to GST-CDK6/GST-D2 complex in the presence of varying amounts of cold A61T as indicated on *top*.

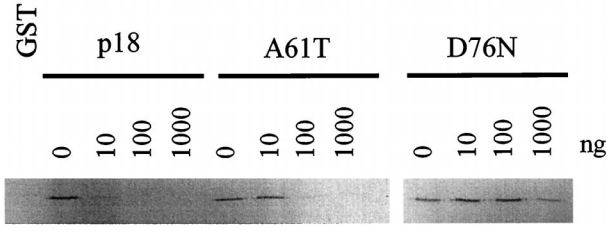

Fig. 5. Cyclin D2 displacement assay. An aliquot of *in vitro* translated, ^{35}S-labeled CDK6 (CDK6*) was mixed with GST (*Lane 1*, from *left* to *right*) or GST-cyclin D2 (*Lanes 2–13*) and increasing concentrations (0, 10, 100, and 1000 ng) of untagged, purified wild-type p18 (*Lanes 2–5*), A61T (*Lanes 6–9*), or D76N (*Lanes 10–13*). The resulting complex was immunoprecipitated using anti-cyclin D1 antibody and resolved on a SDS-polyacrylamide gel for autoradiography.

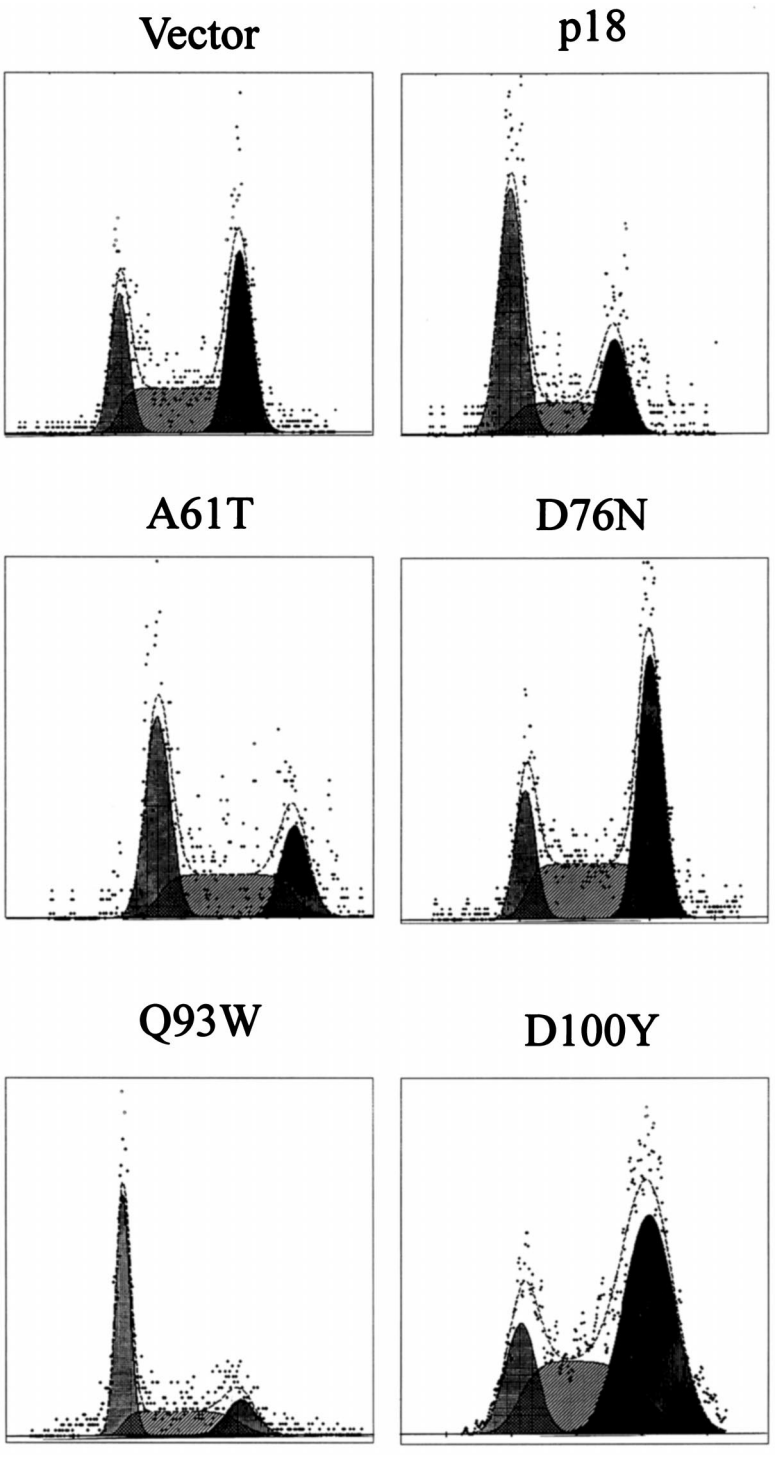

Fig. 6. FACS analysis profiles. Cells transfected with the expression vector containing wild-type p18 or mutant coding sequence (mutant as indicated on *top* of each panel) were analyzed by two parameter FACS analysis. Histograms represent the DNA content of CD20-positive U-2OS cells.

pared to the number of colonies formed on plates of cells transfected with pcDNA3 itself (Table 3). Three independent experiments were performed. Transfection with vector alone produced an average of 37 neomycin-resistant colonies. In contrast, an average of only 4 neomycin-resistant colonies were formed on plates of wild-type p18-transfected cells, confirming that p18 overexpression inhibits the growth and proliferation of the transfected cells. This inhibition is specific for functional p18 expression because plates of cells transfected with antisense p18 formed an average of 39 colonies, similar to the result of transfection by vector alone. Transfection with A61T, which binds well to both CDK4 and CDK6 and retains some inhibitory capacity toward CDK4 and CDK6, caused a reduction in the number of colonies to 16. Although not quite as complete as that with the wild-type p18, A61T did significantly inhibit cell growth and proliferation. Similar results were obtained with Q93W, which binds much less tightly to the CDK molecules than does p18 but retains at least 10% of the inhibitory capacity toward both CDK4 and CDK6. Transfection with D100Y, on the other hand, resulted in similar number of resistant colonies as the vector control. This result further supports the idea that the growth suppression is probably due to the ability of p18 to curtail CDK4/CDK6 activities because D100Y neither binds nor inhibits either of the CDK molecules. Expression of D76N, the mutant that has

Table 2 *FACS analysis summary*[a]

	G_1	S	G_2
Vector	25 ± 7%	44 ± 8%	31 ± 14%
p18	47 ± 7%	29 ± 5%	24 ± 4%
A61T	51 ± 10%	31 ± 6%	18 ± 5%
D76N	29 ± 10%	36 ± 6%	35 ± 6%
Q93W	48 ± 11%	31 ± 5%	21 ± 11%
D100Y	16 ± 0%	33 ± 1%	51 ± 1%

[a] Expression vector (pcDNA3), either empty or containing p18 or mutant, as designated in the first column, was transfected into U-2OS cells. Double-parameter FACS analysis was performed. The numbers in each column represent the percentages of transfection-positive cells (CD20-positive) residing in the indicated stage of cell cycle, as determined by DNA content.

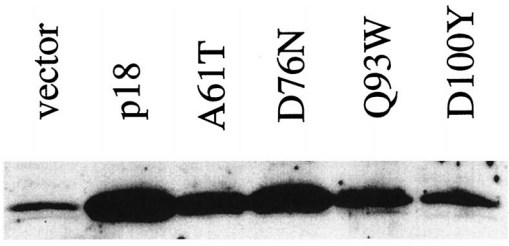

Fig. 7. Western blot of transfection samples. Western blot of the lysates of cells transfected with vector, wild-type p18, or mutants as designated above each lane. A mixture of antisera raised against the NH_2- and COOH-terminal fragments of p18 was used.

completely lost the ability to inhibit either of the two G_1 CDKs but still binds to CDK4, resulted in an average of 16 resistant colonies. This result suggests that D76N is able to inhibit cell proliferation possibly by virtue of binding to one of the two cyclin D-associated CDKs.

DISCUSSION

Although the sequences of INK4 proteins are only ~30% identical, these molecules share the feature that they consist almost exclusively of tandem ankyrin repeats (Fig. 1). These repeats are expected to constitute structural elements critical for the INK4-CDK interactions because ankyrin repeats are known to be involved in molecular recognition (34). The three-dimensional structures of p18 and p19 were recently solved by X-ray crystallography and nuclear magnetic resonance, respectively (35, 36). p18 and p19, as expected, appear to be similar in overall structure. In p18, each ankyrin repeat folds into an NH_2-terminal β-strand followed by two α-helices arranged in antiparallel manner and an extended loop region culminating in a COOH-terminal β-strand. Tight β-turns connect the five ankyrin repeats to form an extended three-dimensional structure. The β-strands of the repeats align to form a β-sheet that is orthogonal to the helical bundle formed by extensive interactions between the α-helices of the five ankyrin repeats (35).

V118 is one of many residues conserved among the INK4 proteins that are thought to stabilize the helical bundle by interrepeat hydrophobic interactions. Substitution of this hydrophobic residue with a charged residue (V118D) did not affect CDK binding very much; however, the mutation did moderately reduce CDK inhibition (Table 1). G16 and G81 occur at the β-turn regions connecting the two α-helices of repeats 1 and 3, respectively (35). Although mutation at G16 had negligible effects on the ability of p18 to bind and inhibit CDK4 and CDK6 (Table 1), G81S caused a 10-fold reduction in CDK6 inhibition. The ability to make a tight turn to correctly align the two helices of the third repeat, therefore, must be important for the inhibitory function of p18. Analysis of the known structures of ankyrin repeats suggested that a proline or alanine residue is preferred at position 5 of an ankyrin repeat to allow the sharp bend between the β-strand and the first α-helix (35). P106 occurs at position 5 of repeat 4. Changing this proline to leucine slightly impaired CDK6 binding and reduced CDK inhibition by at least 10-fold (Table 1; Fig. 2). The importance of proper alignment of the fourth ankyrin repeat with the third repeat is reemphasized by the data for D100Y. D100 occurs at position 32 of repeat 3. This aspartate residue is thought to be involved in a hydrogen-bonding interaction with the second residue of the loop that connects the third and fourth repeat (35). Mutation of this residue to tyrosine abolished all binding and inhibition of p18 to either CDK4 or CDK6. Stabilization of the tight turn linking the third and fourth ankyrin repeats, therefore, seems to be essential for the ability of p18 ability to function as CDK inhibitor. D76 and R79 are solvent exposed residues that occur on the helices of the third repeat that are strictly conserved among the INK4 proteins. It has been speculated that these solvent-exposed residues may be involved in interaction with CDK molecules (35). Mutations of D76 or R79 abolished the CDK inhibitory activity of p18 and also significantly impaired CDK6 and CDK4 binding (Table 1). It seems, therefore, that the solvent exposed, conserved residues of the helices in the third ankyrin repeat of p18 are critical for the ability of p18 to bind and inhibit the CDK4 and CDK6. Additionally, the ability of D76N to bind well to CDK4 but not CDK6 (Fig. 3) suggests that p18 may be using different portions of the solvent-exposed face of the α-helices in the third ankyrin repeat to interact differentially with CDK4 and CDK6.

Saturation binding experiments, which involved binding of p18 to CDK6-cyclin D2 complex, yielded data that are consistent with the results of the *in vitro* binding experiments, in which p18 bound to free CDK6 subunit. Therefore, p18 most likely uses the same interactions to bind to the free and the complexed forms of CDK6. This conclusion is further supported by our observation that p18 competes with cyclin D2 for formation of a binary complex (Fig. 5) and that the ability of p18 mutants to displace cyclin D2 from CDK6 correlates with their CDK6 binding affinity (Figs. 3 and 4). These data suggest that p18 likely inhibits CDK6 by binding to the kinase subunit to the exclusion of cyclin D2, thus preventing activation of the kinase. Additionally, the saturation binding experiments also confirmed the preferential interaction of p18 with CDK6-cyclin D relative to the CDK4-cyclin D complex.

The *in vitro* binding and CDK inhibition data reported in this study agree with previously reported biochemical characterization of analogous p16 mutants. Yang *et al.* (22), for example, reported that G101W (corresponding to Q93W) exhibited reduced binding to CDK4 and was 50–100-fold less potent than wild-type p16 in CDK4 inhibition (22). Substitution of H83 (the residue adjacent to what corresponds to D76 in p18) with tyrosine also reduced binding and completely abolished the ability of p16 to inhibit CDK4 (22). P114L mutant, which corresponds to the P106L mutant of p18 (23), was at least 10-fold less potent than wild-type p16 as CDK4 inhibitor in the hands of Koh *et al.* (23). Lukas *et al.* (13) found that P114L mutant did not bind to either CDK4 or CDK6. The *in vivo* and *in vitro* characterization of D84N, R87P, and H98P, which correspond to D76N, R79P, and H89P (residue just pre-

Table 3 *Summary of the growth inhibition studies*[a]

	Experiment no.		
Transfected DNA	1	2	3
None	0	0	9
pcDNA3	47	24	39
pcDNA3-p18	2	1	9
pcDNA3-p18AS	45	27	46
pcDNA3-A61T	28	10	9
pcDNA3-D76N	17	15	15
pcDNA3-Q93W	14	9	9
pcDNA3-D100Y	70	39	27

[a] Number of G418-resistant colonies surviving in culture after transfection with vector control or expression vector containing p18 or mutant were counted in three separate experiments.

ceding L90P) in p18, were also consistent with our data (23). These corroborating data support the idea that the INK4 family likely share structural features.

The effects of the mutations on the physiological function of p18, namely, to cause G_1 arrest and stop cell growth, were tested using colony formation assay and FACS analysis of transiently transfected cells. By and large, the mutant p18 molecules affected cell cycle distribution and growth properties of U-2OS cells in manner consistent with their biochemical properties. Q93W, the inhibitory and binding capacities of which were very minimally affected, caused accumulation of U-2OS cells at G_1 at levels comparable to the wild-type p18. The CDK4/6-inhibitory activity of A61T but not its binding was adversely affected, and it caused the G_1 accumulation of U-2OS cells at a level comparable to wild-type p18. Both A61T and Q93W also inhibited the formation of G418-resistant colonies in the growth assay, although not as effectively as the wild-type p18. As expected, D100Y, which neither binds nor inhibits the two CDK molecules, did not cause G_1 arrest and did not inhibit the formation of G418-resistant colonies. It is interesting to note that D100Y transfection, in fact, caused a slight accumulation of cells in G_2 and also a mild increase in the number of neomycin-resistant colonies. D100Y may, therefore, possibly be acting as a weak dominant interfering mutant. D76N, on the other hand, yielded some confounding results. Consistent with its inability to inhibit either of the CDK molecules *in vitro*, D76N did not cause accumulation of the transfected U-2OS cells in G_1 (Table 2). When its ability to inhibit cell proliferation was assessed by the colony formation assay, however, D76N was able to partially inhibit colony formation, at the same level as A61T and Q93W. Although D76N can no longer inhibit CDK4 or CDK6, the mutant still binds well to CDK4. This residual binding activity, in the setting of overexpression, may be enough to interfere with active CDK4-cyclin D complex formation, thereby inhibiting cell growth.

In summary, the biochemical properties of the p18 mutants, when analyzed in light of the recently reported three-dimensional structure of p18, suggest that the proper folding of the third ankyrin repeat and the proper alignment of the fourth repeat relative to the third repeat are essential for the ability of p18 to inhibit CDK activity. Mere binding of p18 to CDK, however, does not seem to require such extensive contacts, because the mutation of the second and fourth ankyrin repeat determinants do not affect the ability of p18 to bind to CDK4 or CDK6. The finding that mutation of one of the solvent exposed residues of the first helix in third ankyrin repeat abolished the ability of p18 ability to bind to CDK6 but did not affect CDK4 binding further suggested that p18 may be using slightly different binding elements of the third repeat to discriminate between the two CDK molecules.

ACKNOWLEDGMENTS

We thank Dr. E. Harlow for the pCMV-CD20 plasmid, Dr. E. R. Butch for critical reading of the manuscript, E. Tang for suggestions, and Dr. M. G. Spigarelli for invaluable help in the preparation of this manuscript.

REFERENCES

1. Pines, J. Cyclins and cyclin-dependent kinases: take your partners. Trends Biochem. Sci., *18:* 195–197, 1993.
2. El-Deiry, W. S., Tokino, T., Velculescu, V. V., Levy, D. B., Parsons, R., Trent, J. M., Lin, D., Mercer, E., Kinzler, K. W., and Vogelstein, B. WAF1, a potential mediator of p53 tumor suppression. Cell, *75:* 817–825, 1993.
3. Gu, Y., Turek, C. W., and Morgan, D. O. Inhibition of CDK2 activity *in vivo* by an associated 20K regulatory subunit. Nature (Lond.), *366:* 707–710, 1993.
4. Harper, J. W., Adami, G. R., Wei, N., Keyomarsi, K., and Elledge, S. J. The p21 cdk-interacting protein Cip1 is a potent inhibitor of G1 cyclin-dependent kinases. Cell, *75:* 805–816, 1993.
5. Xiong, Y., Hannon, G. J., Zhang, H., Casso, D., Kobayashi, R., and Beach, D. p21 is a universal inhibitor of cyclin kinases. Nature (Lond.), *366:* 701–704, 1993.
6. Toyoshima, H., and Hunter, T. p27, a novel inhibitor of G1 cyclin/cdk protein kinase activity, is related to p21. Cell, *78:* 67–74, 1994.
7. Serrano, M., Hannon, G. J., and Beach, D. A new regulatory motif in cell cycle control causing specific inhibition of cyclin D/cdk4. Nature (Lond.), *366:* 704–707, 1993.
8. Guan, K. L., Jenkins, C. W., Li, Y., Nichols, M. A., Wu, X., O'Keefe, C. L., Matera, A. G., and Xiong, Y. Growth suppression by p18, a $p16^{INK4/MTS2}$-related CDK6 inhibitor, correlates with wild-type pRb function. Genes Dev., *8:* 2939–2952, 1994.
9. Hannon, G. J., and Beach, D. $p15^{INK4b}$ is a potential effector of cell cycle arrest mediated by TGF-β. Nature (Lond.), *371:* 257–261, 1994.
10. Chan, F. K. M., Zhang, J., Chen, L., Shapiro, D. N., and Winoto, A. Identification of human/mouse p19, a novel cdk4/cdk6 inhibitor with homology to $p16^{ink4}$. Mol. Cell. Biol., *15:* 2682–2688, 1995.
11. Hirai, H., Roussel, M. F., Kato, J., Ashmun, R. A., and Sherr, C. J. Novel INK4 proteins, p19 and p18, are specific inhibitors of cyclin D-dependent kinases CDK4 and CDK6. Mol. Cell. Biol., *15:* 2672–2681, 1995.
12. Guan, K. L., Jenkins, C. W., Li, Y., O'Keefe, C. L., Noh, S., Wu, X., Zariwala, M., Matera, A. G., and Xiong, Y. Isolation and characterization of p19INK4d, a p16-related inhibitor specific to CDK6 and CDK4. Mol. Biol. Cell., *7:* 57–70, 1996.
13. Lukas, J., Parry, D., Aagaard, L., Mann, D. J., Bartkova, J., Strauss, M., Peters, G., and Bartek, J. Retinoblastoma protein-dependent cell-cycle inhibition by the tumor suppressor p16. Nature (Lond.), *375:* 503–506, 1995.
14. Tam, S. W., Shay, J. W., and Pagano, M. Differential expression and cell cycle regulation of the cyclin-dependent kinase 4 inhibitor $p16^{ink4}$. Cancer Res., *54:* 5816–1820, 1994.
15. Kamb, A., Gruis, N. A., Weaver-Feldhaus, J., Liu, Q., Harshman, K., Tavtigian, S. V., Stockert, E., Day, R. S., III, Johnson, B. E., and Skolnick, M. H. A cell cycle regulator potentially involved in genesis of many tumor types. Science (Washington DC), *264:* 436–440, 1994.
16. Caldas, C., Hahn, S. A., da Costa, L. T., Redston, M. S., Schutte, M., Seymour, A. B., Weinstein, C. L., Hruban, R. H., Yeo, C. J., and Kern, S. E. Frequent somatic mutations and homozygous deletions of the *p16* (*MTS1*) gene in pancreatic adenocarcinoma. Nat. Genet., *8:* 27–32, 1994.
17. Hussussian, C. J., Struewing, J. P., Goldstein, A. M., Higgins, P. A. T., Ally, D. S., Sheahan, M. D., Clark, W. H., Jr., Tucker, M. A., and Dracopoli, N. C. Germline p16 mutations in familial melanoma. Nat. Genet., *8:* 15–21, 1994.
18. Kamb, A., Shattuck-Eidens, D., Eeles, R., Liu, Q., Gruis, N. A., Ding, W., Hussey, C., Tran, T., Miki, Y., Weaver-Feldhaus, J., McClure, M., Aitken, J. F., Anderson, D. E., Bergman, W., Frants, R., Goldgar, D. E., Green, A., MacLennan, R., Martin, N. G., Meyer, L. J., Youl, P., Zone, J. J., Skolnick J. H., and Cannon-Albright, L. A. Analysis of the *p16* gene (CDKN2) as a candidate for the chromosome 9p melanoma susceptibility locus. Nat. Genet., *8:* 22–26, 1995.
19. Moulton, T., Samara, G., Chung, W-Y., Yuan, L., Desai, R., Sisti, J., Bruce, J., and Tycko, B. MTS1/p16/CDKN2 lesions in primary glioblastoma multiforme. Am. J. Pathol., *146:* 613–619, 1995.
20. Quesnel, B., Preudhomme, C., Philippe, H., Vanrumbeke, M., Dervite, I., and Lai, J. L. *p16* gene homozygous deletions in acute lymphoblastic leukemia. Blood, *85:* 657–663, 1995.
21. Washimi, O., Nagatake, M., Osada, H., Ueda, R., Koshikawa, T., Seki, T., Takahashi, T., and Takahashi, T. *In vivo* occurrence of p16 (MTS1) and p15 (MTS2) alterations preferentially in non-small cell lung cancers. Cancer Res., *55:* 514–517, 1995.
22. Yang, R., Gombart, A. F., Serrano, M., and Koeffler, H. P. Mutational effects on the $p16^{INK4a}$ tumor suppressor protein. Cancer Res., *55:* 2503–2506, 1995.
23. Koh, J., Enders, G. H., Dynlacht, B. D., and Harlow, E. Tumour-derived *p16* alleles encoding proteins defective in cell-cycle inhibition. Nature (Lond.), *375:* 506–510, 1995.
24. Parry, D., and Peters, G. Temperature-sensitive mutants of p16CDKN2 associated with familial melanoma. Mol. Cell. Biol., *16:* 3844–3852, 1996.
25. Reymond, A., and Brent, R. p16 proteins from melanoma-prone families are deficient in binding to Cdk4. Oncogene, *11:* 1173–1178, 1995.
26. Zhang, B., and Peng, Z-Y. Defective folding of mutant p16(INK4) proteins encoded by tumor-derived alleles. J. Biol. Chem., *271:* 28734–28737, 1996.
27. Gemma, A., Takenoshita, S., Hagiwara, K., Okamoto, A., Spillare, E. A., McMemamin, M. G., Hussain, S. P., Forrester, K., Zariwala, M., Xiong, Y., and Harris, C. C. Molecular analysis of the cyclin-dependent kinase inhibitor genes *p15INK4b*/*MTS2*, *p16INK4*/*MTS1*, *p18* and *p19* in human cancer cell lines Int. J. Cancer, *68:* 605–611, 1996.
28. Rusin, M. R., Okamoto, A., Chorazy, M., Czyzewski, K., Harasim, J., Spillare, E. A., Hagiwara, K., Hussain, S. P., Xiong, Y., Demetrick, D. J., and Harris, C. C. Intragenic mutations of the *p16*(*INK4*), *p15*(*INK4B*) and *p18* genes in primary non-small-cell lung cancers. Int. J. Cancer, *65:* 734–739, 1996.
29. Guan, K. L., and Dixon, J. E. Eukaryotic proteins expressed in *Escherichia coli*: an improved thrombin cleavage and purification procedure of fusion proteins with glutathione *S*-transferase. Anal. Biochem., *192:* 262–267, 1991.
30. Meyerson, M., and Harlow, E. Identification of a G1 kinase activity for cdk6, a novel cyclin D partner. Mol. Cell. Biol., *14:* 2077–2086.
31. Zhu, L., van den Heuvel, S., Helin, K., Fattaey, A., Ewen, M., Livingston, D., Dyson, N., and Harlow, E. Inhibition of cell proliferation by p107, a relative of the retinoblastoma protein. Genes Dev., *7:* 1111–1125, 1993.
32. Parry, D., Bates, S., Mann, D. J., and Peters, G. Lack of cyclin D-Cdk complexes in Rb-negative cells correlates with high levels of p16INK4/MTS1 tumour suppressor gene product. EMBO J., *14:* 503–511, 1995.
33. Ragione, F. D., Russo, G. L., Oliva, A., Mercurio, C., Mastropietro, S., Pietra, V. D., and Zappia, V. J. Biol. Chem., *271:* 15942–15949, 1996.
34. Michaely, P., and Bennett, V. The ANK repeat: a ubiquitous motif involved in macromolecular recognition. Trends Cell Biol., *2:* 127–129, 1992.
35. Venkataramani, R., Swaminathan, K., and Marmorstein, R. Crystal structure of the CDK4/6 inhibitory protein $p18^{INK4c}$ provides insights into ankyrin-like repeat structure/function and tumor-derived p16INK4 mutations. Nat. Struct. Biol., *5:* 74–81, 1998.
36. Luh, F. Y., Archer, S. J., Domaille, P. J., Smith, B. O., Owen, D., Brotherton, D. H., Raine, A. R., Xu, X., Brizuela, L., Brenner, S. L., and Laue, E. D. Structure of the cyclin-dependent kinase inhibitor $p19^{Ink4d}$. Nature (Lond.), *389:* 999–1003, 1997.

Identification of Functional Elements of p18^{INK4C} Essential for Binding and Inhibition of Cyclin-dependent Kinase (CDK) 4 and CDK6

Seong J. Noh, Yan Li, Yue Xiong, et al.

Cancer Res 1999;59:558-564.